PAPER

Combating selective ionization in the high resolution mass spectral characterization of complex mixtures†

Ryan P. Rodgers, [ID] *[abc] Mmilili M. Mapolelo, [ID] [d]
Winston K. Robbins, [ID] [b] Martha L. Chacón-Patiño, [ID] [a]
Jonathan C. Putman, [ID] [c] Sydney F. Niles, [ID] [c] Steven M. Rowland[ab]
and Alan G. Marshall [ID] [ac]

Direct "dilute and shoot" mass spectral analysis of complex naturally-occurring mixtures has become the "standard" analysis in environmental and petrochemical science, as well as in many other areas of research. Despite recent advances in ionization methods, that approach still suffers several limitations for the comprehensive characterization of compositionally complex matrices. Foremost, the selective ionization of highly acidic (negative electrospray ionization ((−) ESI)) and/or basic (positive electrospray ionization ((+) ESI)) species limits the detection of weakly acidic/basic species, and similar issues (matrix effects) complicate atmospheric pressure photo-ionization (APPI)/atmospheric pressure chemical ionization (APCI) analyses. Furthermore, given the wide range of chemical functionalities and structural motifs in these compositionally complex mixtures, aggregation can similarly limit the observed species to a small (10−20%) mass fraction of the whole sample. Finally, irrespective of the ionization method, the mass analyzer must be capable of resolving tens-of-thousands of mass spectral peaks and provide the mass accuracy (typically 50−300 ppb mass measurement error) required for elemental composition assignment, and thus is generally limited to high-field Fourier transform ion cyclotron mass spectrometry (FT-ICR MS). Here, we describe three approaches to combat the above issues for (+) ESI, (−) ESI, and (+) APPI FT-ICR MS analysis of petroleum samples. Each approach relies on chromatographic fractionation to help reduce selective ionization discrimination and target either specific chemical functionalities (pyridinic and pyrrolic species (nitrogen) or carboxylic acids (oxygen)) or specific structural motifs (single aromatic core (island) or multi-core aromatics (archipelago)) known to be related to ionization efficiency. Each fractionation method

aNational High Magnetic Field Laboratory, Florida State University, Tallahassee, FL, USA. E-mail: rodgers@magnet.fsu.edu

bFuture Fuels Institute, Florida State University, 1800 East Paul Dirac Drive, Tallahassee, FL, USA

cDepartment of Chemistry and Biochemistry, Florida State University, Tallahassee, FL, USA

dBotswana Institute for Technology Research and Innovation, Gaborone, Botswana

† Electronic supplementary information (ESI) available. See DOI: 10.1039/c9fd00005d

yields a 2–10-fold increase in the compositional coverage, exposes species that are undetectable using direct "dilute and shoot" analysis, and provides coarse selectivity in chemical functionalities that can both increase the assignment confidence and optimize ionization conditions to maximize compositional coverage.

Introduction

Fossil fuels are immensely complex organic mixtures in terms of the number of chemically distinct components.[1–3] Variations in this complexity are of significant interest, because the composition determines their economic value and behavior. Thus, detailed characterization of molecular structure and chemical functionality in fossil fuels is paramount in all segments of the petroleum industry: exploration, production, and refining.[4] Due to the compositional complexity and inability of GC-based techniques to analyze high-boiling petroleum components, the compositions of most petroleum fractions that boil at temperatures above light gas oil (LGO, ~342 °C) are not yet completely defined.[4] Recent advances in ionization techniques, combined with the performance of high magnetic field FT-ICR mass spectrometry, have led to an increased molecular-level understanding of complex, high-boiling petroleum fractions.[5–7] However, several reports have outlined the problems associated with selective ionization and/or matrix effects that can occur prior to mass spectral detection.[8–12] Those effects limit the accessible compositional information in petroleum-derived samples and other complex systems by direct analysis, and pose a significant hurdle to a comprehensive understanding of petroleum composition and its impact on behavior in exploration, production, and refining. Thus, there is an ever-increasing need for chromatographic fractionation methods designed to both separate suspected chemical functionalities/structural motifs prior to mass spectral analysis and overcome the limitations (selectivity) of current ionization methods. Traditionally, separation prior to analysis is carried out by use of chemical class separation schemes that involve combinations of selective solubility, extractions and column chromatography.[13,14] The schemes for the separations vary, but are most often driven by chemical functionality (*i.e.* acids, bases and neutrals) followed by chemical group-type (compound class) fractionation. Generally, most separations are designed for ultimate resolution of chemical functionality/group-types without regard to the ionization method used for subsequent mass spectral analysis.[4]

Heteroatom-containing petroleum compounds have long been of interest to the petroleum industry because they are believed to have a significant role in catalyst deactivation, refinery corrosion problems, formation of deposits, and storage instability during upstream and downstream operations.[15,16] Thus, it is of the utmost importance to characterize the heteroatom-containing fractions in petroleum in order to provide insight into the origin of these species with respect to their biological precursors and their compositional dependence/correlation to upstream and downstream problems. Such insight provides an understanding of physiochemical transformations of the biomolecules in maturation into heteroatom-containing species currently found in petroleum and provides invaluable compositional information that can be used for remediation/prevention strategies.[16] It is most commonly termed the "polar fraction",

because it is isolated with solvents of higher polarity than heptane and toluene, and it is enriched in nitrogen (N), oxygen (O), and sulfur (S) containing molecular species.[13,17–19] Recently, there has been increased interest in the characterization of heteroatom-containing compounds/fractions in petroleum feedstocks, specifically those containing N, S, and O, as well as asphaltenes (the *n*-alkane-insoluble, but toluene-soluble fraction of petroleum).[20–29] Petroleum crude oils are typically composed of ~0.1–2% wt of organic nitrogen compounds, ~0.1–6% wt organic sulfur compounds, ~0.1–1.5% wt organic oxygen compounds, and ~0.1 to 19% wt asphaltenes.[30–32] Nitrogen compounds in petroleum-derived streams are mostly alkylated heterocycles with a predominance of neutral nitrogen (pyrrolic) structures over the basic nitrogen (pyridinic) forms.[33,34] Sulfur compounds consist of thiophenic structures (aromatic), linear/cyclic/aromatic sulfides, and mercaptans.[35–37] Oxygen compounds are more functionally diverse, and consist of carboxylic acids, ketones, aldehydes, alcohols, and furanic heterocycles.[38] Asphaltenes are a solubility class of petroleum that is enriched in aromatics and heteroatoms. It is an ultra-complex fraction of crude oil that contains many, if not all, of the chemical functionalities listed above.[39–43]

The higher boiling point of all heteroatom-containing species due to N, S, and O addition, combined with their high compositional complexity, limits characterization by GC-based techniques.[25] Thus, advances in the characterization of these species has been led by high resolution mass spectrometry.[44–51] Despite these advances, many fundamental questions remain unanswered. First, since mass spectral signal-to-noise is not always directly related to the concentration of a specific analyte in the solution (due to ionization efficiency differences and matrix effects), the overall coverage of the total compositional range captured in the mass spectral data is unknown. Recent results suggest that direct "dilute and shoot" analysis of complex petroleum samples can capture as little as 10% of the overall compositional complexity, representing less than 15 wt% of the sample.[52–54] Proper selection of the ionization method can ease the impact of selective ionization, but only subsequent fractionation followed by mass spectral analysis of all fractions provides a measure of the effectiveness. Most researchers in the field do not perform such analyses, due to the additional expense and effort involved. Moreover, the impact of selective ionization within a chemical functionality class (*i.e.* carboxylic acids) has largely been ignored, but can similarly limit the compositional coverage to levels noted above.[52,55] Thus, even within a chemical functionality class, separations are crucial. Finally, as discussed above, aggregation can severely restrict the compositional information attained from direct (whole) sample analysis. Although recently discussed for asphaltene analysis, the topic requires further investigation (see below).

Gas chromatography (GC) separates heteroatom-containing compounds according to boiling point, whereas liquid chromatography (LC) can serve to separate with respect to polarity and/or hydrophobicity (carbon number). Thus, prior separation of heteroatom-containing compounds by LC has the potential not only to simplify mass spectrometric analysis, but also to address selective ionization in the ion source. Schemes for separating nitrogen compounds into well-defined compound classes have been used to eliminate some of the ambiguities, and therefore assist in compound identification by MS.[56] Here, water is added to the oven-dried stationary phase to deactivate highly active sites. The water increases the loading capacity of the stationary phase at the expense of high

selectivity to further optimize the separation for ESI mass spectral analysis (the separation of components with widely different chemical functionality or polarity). Clinching evidence of the identification and partial recovery of the lost selectivity of the stationary phase is provided by exploiting the selectivity of ESI. Pyridinic (basic) nitrogen is readily detected as $[M + H]^+$ by protonation, whereas pyrrolic (neutral) nitrogen species are detected as $[M - H]^-$ by deprotonation.[21,24] Thus, polarity-based separation combined with selective ionization facilitates detection and differentiation between the 2 major forms of nitrogen functionalities in petroleum. Hydrophobicity-based separation strategies further assist in selective ionization within a chemical functionality class, because they separate by carbon number (molecular weight).[52,55] Finally, extrography fractionation can separate structural motifs (island (single pericondensed aromatic core) *vs.* archipelago (multiple alkyl-linked aromatic cores)) in asphaltene samples that exhibit wide variation (∼50-fold) difference in ionization efficiency.[54,57,58] All three approaches expand the compositional coverage relative to direct (unfractionated) sample analysis and identify species that were not previously accessible.

Here, we describe three separations that can help overcome selective ionization in the analysis of petroleum samples: (1) a column chromatography method that fractionates deasphalted crude oils into four well-defined fractions that can be classified as nonpolar and polar fractions. The column separation unequivocally separates the two main types of nitrogen compounds found in crude oils. The separation affords chemical class separation of polar species according to aromaticity, polarity, and molecular weight prior to FT-ICR MS analysis. (2) a modified aminopropyl silica (MAPS) fractionation that first retains acidic species and subsequently separates them by hydrophobicity (degree of alkylation/ carbon number) for mass spectral analysis. (3) An extrography fractionation method that employs silica gel as the stationary phase that selectively targets the removal of asphaltene species that have high ionization efficiencies relative to other asphaltene species. Removal of these species facilitates detection of less efficiently ionized species that are not observable in the analysis of the whole asphaltene sample. The ionization efficiency differences are related to molecular structure and tendency to aggregate.[54]

Materials and methods

Samples and preparation

Three crude oils of different geographical origin were used as supplied. The crude oil properties are provided in Table 1. MacKay bitumen is highly degraded with high sulfur (S), moderate nitrogen (N) and high oxygen (O) (naphthenic acid) content.[59] South American crude oils are typically rich in both S and N with complex "bottoms", whereas the Central American "Maya" crude oil is sulfur-rich

Table 1 General properties of the parent crude oils

Sample	Origin	Crude oil (API gravity @ 15 °C, TAN)
Maya crude oil	Central America	21.3°, 0.3 mg KOH per g oil
South American crude oil	South America	25.9°, 0.70 mg KOH per g oil
MacKay bitumen	Canada	8.0°, 2.49 mg KOH per g oil

but has a low nitrogen content.[60,61] The South American crude oil was used for the nitrogen separation, MacKay bitumen for the MAPS fractionation, and Maya crude oil asphaltenes for the extrography separation. HPLC grade n-heptane, toluene, tetrahydrofuran and methanol (J.T. Baker), Whatman No. 1 filter paper (Fisher Scientific), deionized water, silicic acid n-hydrate powder, and anhydrous sodium sulfate (Na_2SO_4) (J.T. Baker), sand (white quartz $-50 + 70$ mesh), chromatographic grade silica gel (100–200 mesh, type 60 Å, Fisher Scientific), glass wool, ammonium hydroxide (NH_4OH) (20–35% ammonia in water), formic acid (HCOOH) and tetramethylammonium hydroxide [TMAH ($(CH_3)_4N^+OH^-$)] (Sigma-Aldrich) were used as supplied.

Preparation of 10% water-deactivated silicic acid and column packing

100 g of silicic acid n-hydrate powder was oven-dried (activated) at 120–140 °C overnight. The activated silicic acid was allowed to cool in a desiccator. To deactivate the silicic acid, 90 g of the dry silicic acid was combined with 10 mL of deionized water. The deactivated silicic acid was put in a wide-mouthed jar, agitated to eliminate lumps and allowed to equilibrate overnight. Sixty grams of deactivated silicic acid was mixed with 100 mL of n-heptane to make a slurry. The slurry was kept well-mixed and poured into a chromatographic column (25 × 300 mm) fitted with a 300 mL glass reservoir at its top and a medium glass frit and stopcock at its bottom. The excess n-heptane was allowed to drain through the stopcock until the solvent level reached the top of the stationary phase. Once all of the deactivated silicic acid had settled into the column, the sides of the column were rinsed with n-heptane, leaving several inches of solvent above the deactivated silicic acid stationary phase. Approximately 12 g (1/2 inch) of sand was added on top of the packed deactivated silicic acid stationary phase, followed by an additional wad of glass wool. About 2 mL of n-heptane was left above the top of the glass wool. The column could be dry-packed; however, better resolution and a more consistent behavior can be achieved through the slurry packing technique. The slurry packing eliminates air pockets and uneven flow down the column. The sand and glass wool at the column top allow move even distribution during loading of the sample.

Asphaltene precipitation and isolation

10 g of each of the two crude oils (South American and MacKay bitumen) was deasphalted via precipitation of asphaltenes in an excess of saturated hydrocarbon solvent (n-heptane) (40 : 1) prior to chromatographic separation. A Whatman No. 1 filter paper was used to separate and collect the n-heptane insolubles (asphaltenes) from the n-heptane solubles (maltenes). All of the n-heptane solubles washings were combined and the maltene solution reduced to 5 mL. Isolation and extrography fractionation of Maya asphaltenes are discussed below.

Silicic acid sample separation

2–2.5 g of the maltenes were loaded onto the column. The flow rate of the column was adjusted to ~2.5 mL min^{-1}. Components of the crude oils were selectively eluted by use of solvents of increasing polarity ($i.e.$, solvent strength). The most polar components are adsorbed on the active sites of the stationary phase

(adsorbent) and the less polar compounds are least retained by the stationary phase. Four fractions were collected in the following elution order; hydrocarbons (non-polar), neutral nitrogen, basic nitrogen, and polars. Hydrocarbons (HC) were eluted with 250 mL of 90 : 10 (vol : vol) n-heptane : toluene. The neutral nitrogen fraction (neutral N) was eluted with 200 mL of 50 : 50 (vol : vol) n-heptane : toluene, whereas the basic nitrogen fraction (basic N) was eluted with 200 mL of 90 : 10 (vol : vol) toluene : methanol. The polars fraction (polars) was eluted with 200 mL of 85 : 15 (vol : vol) methanol : toluene. To overcome overlap between the different fractions, intermediate fractions were collected between fractions when the new eluent (different mobile phase composition) flowed down the column. The methanol used in the elution of the polar fraction did strip some of the water from the column. However, the water was removed by filtration of the fraction through a bed of anhydrous Na_2SO_4. The excess solvent in the collected fractions was reduced by evaporation, and the weights of the dry fractions were recorded (see Table 2). A schematic representation of the separation is shown in Fig. S1.†

MAPS fractionation

Deasphalted MacKay bitumen was isolated as described above and dried under a stream of dry nitrogen gas. The APS and MAPS fractionation were performed as previously described.[52] The first six fractions were analyzed (MA1–MA6).

Asphaltene extrography fractionation

10 g of Maya crude oil was mixed with 400 mL of heptane (dropwise added, with sonication at 60 °C). After 12 h, solids were collected by filtration and Soxhlet-extracted with heptane until the solvent appeared colorless (∼84 h). Asphaltenes were recovered *via* dissolution with hot toluene, and dried with N_2. Further asphaltene cleaning was conducted by use of a method reported elsewhere.[62] In short, asphaltene solids were crushed and Soxhlet-extracted with heptane; this cleaning cycle was repeated four times to decrease the concentration of occluded/entrained maltenes. Subsequently, cleaned asphaltenes were adsorbed on silica gel (0.5% mass loading). The resulting solid material was Soxhlet-extracted with acetone, followed by toluene and (1 : 1 vol : vol) toluene/THF. The extraction with each solvent lasted 24 h. Fractions were dried under N_2 and stored in the dark for

Table 2 Weight yield of various fractions from silicic acid chromatographic separation of the parent crude oil[a]

Crude oil	South American (g)
Hydrocarbons (HC)	1.4922
Intermediate HC–NN	0.0122
Neutral nitrogen (NN)	0.0874
Intermediate NN–BN	0.0048
Basic nitrogen (BN)	0.0270
Polars (PLR)	0.0287

[a] All weights are based on loading 2 g of deasphalted parent crude oils onto the column.

MS analyses. The whole asphaltene and extrography fractions are denoted whole, acetone, toluene, and Tol/THF.

Sample preparation for ESI FT-ICR MS

Sample preparation for the analysis of asphaltene, polar acidic, and polar basic species in petroleum and petroleum-derived materials by atmospheric pressure photo-ionization and negative-ion/positive-ion electrospray FT-ICR MS has been previously reported.[53,63] Samples were analyzed at a concentration of 50–500 µg mL^{-1} in a standard ESI spray mix (50 : 50 (vol : vol) toluene : methanol) or toluene (APPI) for mass spectrometric analysis. For (−) ESI nitrogen species analyses, a representative aliquot (1 mL) of each fraction was spiked with 10 µL of 2% TMAH in methanol to facilitate the deprotonation of the acidic species to generate [M − H]$^-$ ions, whereas 10 µL of 2% HCOOH in methanol was used to protonate the basic species to generate [M + H]$^+$ ions. TMAH increases the degree of ionization of slightly acidic nitrogen-containing classes relative to ESI with NH$_4$OH.[64] Acidic APS and MAPS (MA1–MA4) fractions were analyzed at concentrations of 10–250 µg mL^{-1} in (50 : 50 (vol : vol)) toluene : methanol with 0.1% vol NH$_4$OH. Due to poor ionization, the concentration of NH$_4$OH was increased to 0.2% vol for the analysis of fraction MA5, and MA6 performed so poorly even under standard conditions that the solvent system and modifier required further optimization. For MA6, they were changed to 250 µg mL^{-1} in (50 : 50 (vol : vol)) DCM : methanol with 0.125% vol TMAH. Whole Maya asphaltenes and the extrography fractions were diluted in toluene at 200 µg mL^{-1} for positive-ion APPI.

Mass analysis

Each sample was analyzed with a custom-built 9.4 T 22 cm horizontal room temperature bore diameter (Oxford Corp., Oxford Mead, UK) FT-ICR mass spectrometer at the National High Magnetic Field Laboratory.[65] A Predator data system was used to acquire and process ICR data.[65,66] All elemental composition assignments and subsequent data processing were performed with PetroOrg.[67] Mass spectrometer parameters and protocols are similar to those previously described.[52–54,57,68,69]

Results and discussion

Nitrogen separation

LC-MS allows us to address important issues in heavy hydrocarbon characterization, including (i) differentiation of alkyl-aromatics from naphtheno-aromatics, (ii) distinction between aromatic hydrocarbons and thiophenes, (iii) analysis of basic and neutral polars, and (iv) correlation of molecular polarity based on elution characteristics in different chromatographic fractions.[56,70] Silicic acid chromatographic separation was developed to fractionate polar compounds with two main types of nitrogen compounds in shale oils, particularly in shale high vacuum gas oils (HVGO), *i.e.*, pyrrole and pyridine benzologs.[14] Mechanistically, a layer of water supported by silicic acid provides an inherently acidic stationary phase surface that separates polar molecules based on differences in their ability to hydrogen-bond. Thus, it retains basic nitrogen functionalities (proton acceptors) more effectively than neutral nitrogen functional groups

(proton donors), thereby separating the benzologs of pyrrole from those of pyridine. Highly alkylated compounds, such as N-alkylated pyrroles, exhibit very little H-bonding. They elute as or with the aromatics, because adsorption by nitrogen occurs perpendicularly at the edge of the molecule, and retention is limited by steric accessibility.

Mass spectral data interpretation

Petroleum feedstocks are composed mainly of homologous series, $C_cH_{2c+z}X$, in which c is the carbon number, z is the "hydrogen deficiency" index, and X denotes heteroatoms (N, S, and O) in each molecule, and successive members of the series differ by multiples of CH_2.[71] Although hydrogen deficiency provides a measure of aromaticity, each ring or double bond contributes -2, and $z = +2$ for a fully saturated hydrocarbon. Thus, a more accurate index is double bond equivalents (DBE), defined as the number of rings plus double bonds involving carbon for a molecular elemental composition,[72,73] $C_cH_hN_nO_oS_s$:

$$\text{Double Bond Equivalents (DBE)} = c - \frac{h}{2} + \frac{n}{2} + 1 \tag{1}$$

The two parameters are related by:

$$z = -2\text{DBE} + n + 2 \text{ or equivalently, DBE} = -z/2 + n/2 + 1 \tag{2}$$

We highlight the broadband ESI mass spectra of a South American crude oil and its respective fractions to illustrate the molecular weight distribution and compositional complexity. We further analyze the individual heteroatom classes for the separated polar nitrogen compounds. Furthermore, each class is sorted according to DBE and carbon number to reveal patterns of aromaticity and alkylation that help to define their core structures and provide a visual indicator of the compositional coverage achieved for the whole and/or chromatographic fractions. Finally, for all three separation methods, we present monomer ion yields (MIY, a measure of ionization efficiency) to highlight the impact of selective ionization for the analysis of these complex samples.[53] MIY is the inverse of the product of ion accumulation period and analyte concentration required to reach a target number of ions. Thus, a low monomer ion yield value indicates poor ionization efficiency. When possible, all related samples and their respective fractions are analyzed at the same sample concentration.

$$\text{MIY} = 1/[(\text{accum. period})(\text{analyte concentration})] \tag{3}$$

Basic nitrogen characterization by (+) ESI FT-ICR MS

The crude oil and its respective fractions were analyzed by positive-ion ESI FT-ICR MS to highlight trends in the basic nitrogen (pyridinic) species from the fractionated South American crude oil. Fig. 1 summarizes the DBE and carbon number compositional images for the four major heteroatom classes (N_1, N_1S_1, N_2, and N_1O_1) along with their relative abundances (R.A.) from the (+) ESI FT-ICR MS analysis. Each heteroatom specific image is composed of thousands of basic

(+) ESI 9.4 T FT-ICR MS
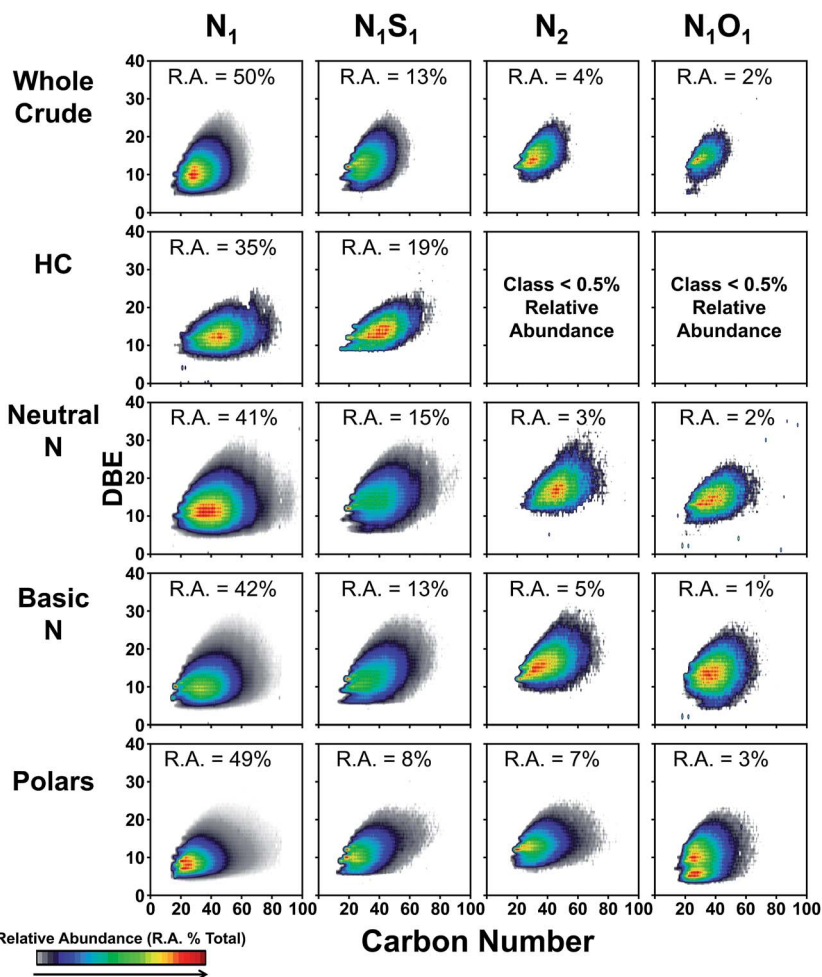
South American Crude Oil

Fig. 1 Isoabundance-contoured isoabundance plots of double bond equivalents (DBE) *versus* carbon number from the (+) ESI FT-ICR MS analysis (pyridinic nitrogen) of the whole deasphalted South American crude oil and its hydrocarbon (HC), neutral nitrogen, basic nitrogen, and polars fractions obtained from silicic acid column chromatography for the four most abundant classes (N_1, N_1S_1, N_2, and N_1O_1) detected in the whole crude oil analysis.

species, predominately nitrogen (N_x species) and nitrogen heteroatom-containing (N_xO_y or N_xS_y) compounds. The fractionation clearly extends the molecular weight distributions of the hydrocarbon and neutral nitrogen fractions (carbon numbers 20–90) beyond the molecular weight distribution of the parent crude (carbon numbers 20–60), and thereby enables the identification of higher molecular weight species unobservable in the parent crude oil. As the fractionation progresses from the HC to the neutral N, basic N, and finally the polars, the DBE and carbon number ranges steadily decline. Thus, the least-retained species have the

highest carbon numbers (most sterically hindered) and are the most alkylated N_1 and N_1S_1 species. Unsurprisingly, the molecular weight (carbon number) and DBE ranges for the basic nitrogen and polar fraction more closely resemble those for the parent crude (carbon numbers 20–60), given the monomer ion yield data presented in Fig. 2. The basic N and polars fractions display monomer ion yields between 3- and 10-fold higher than those for the preceding hydrocarbons and neutral N fractions. Thus, without fractionation, the basic N and polars species dominate the ionization process and limit detection of the compositional information found in the hydrocarbons and neutral N fractions (higher carbon number species). Hence, the chromatographic separation gives a broader class composition (carbon number and DBE) and eliminates ambiguities such as isobaric interferences, and somewhat reduces the effects of selective ionization. The preferential ionization of lower molecular weight (lower carbon number) species in complex petroleum samples is a reoccurring theme, as discussed below for the analysis of neutral nitrogen (with this separation method) and acidic (oxygen-containing) species (in MAPS fractionation).

Neutral nitrogen characterization by −ESI FT-ICR MS

The same fractions summarized in Fig. 1 ((+) ESI) were analyzed using (−) ESI FT-ICR MS to highlight trends in neutral nitrogen (pyrrolic) species. Fig. 3 summarizes the compositional information for the whole crude and the HC, neutral N, basic N, and polars fractions for neutral nitrogen (pyrrolic) species and reveals trends similar to those previously observed in the analysis of the pyridinic species using +ESI. Most notably, the HC and neutral nitrogen fraction contain the highest molecular weight (carbon number) species, and, as the fractionation progresses to the basic N and polars fractions, the N_1 and N_1S_1 class species rapidly drop to lower carbon number values but maintain roughly the same DBE range (10 < DBE < 30). As for the previous analysis of pyridinic species (basic N), the compositional information obtained in the whole crude analysis most closely matches the species that are selectively ionized by the respective ESI mode (±). In the previous discussion, it was the basic nitrogen (pyridinic species) fraction for
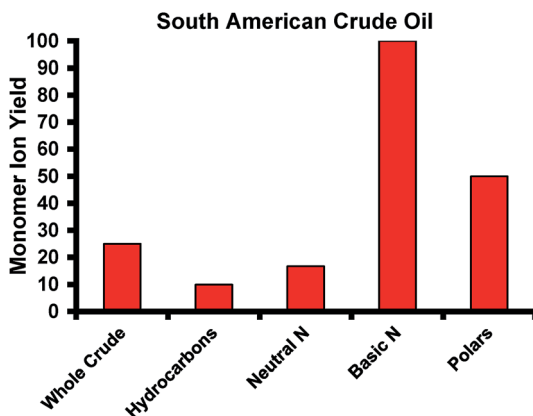

Fig. 2 Monomer ion yield for the whole deasphalted oil and hydrocarbon (HC), neutral nitrogen, basic nitrogen, and polars fractions obtained from silicic acid fractionation of South American crude oil.

(-) ESI 9.4 T FT-ICR MS
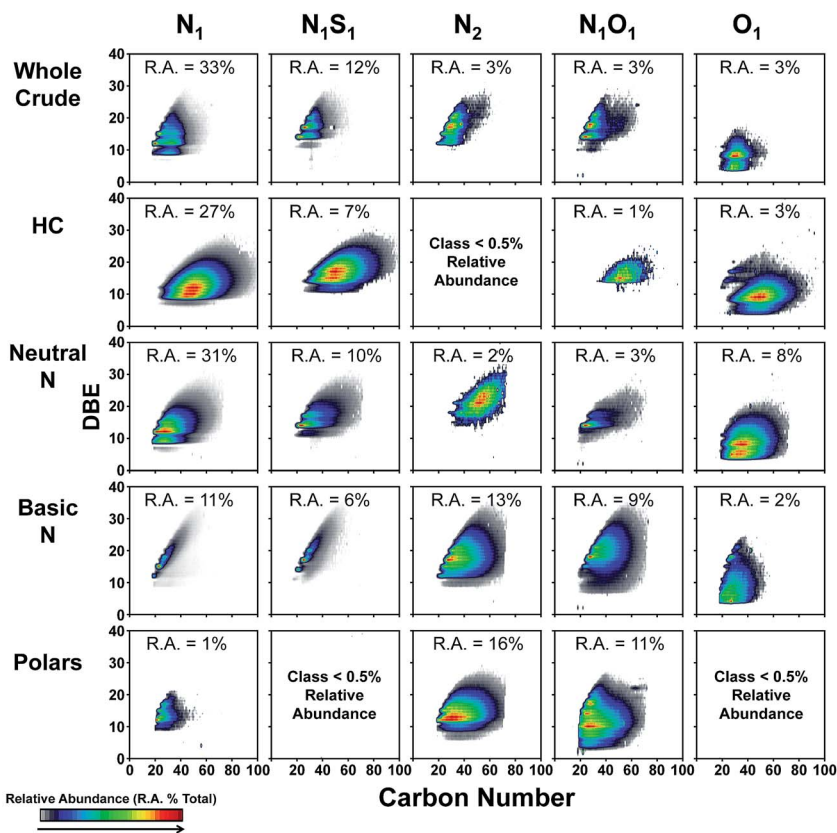
South American Crude Oil

Fig. 3 Isoabundance-contoured plots of DBE *versus* carbon number from (−) ESI FT-ICR MS analysis (pyrrolic nitrogen) of the whole deasphalted South American crude oil and its hydrocarbon (HC), neutral nitrogen, basic nitrogen, and polars fractions obtained from silicic acid column chromatography for the 5 most abundant classes (N_1, N_1S_1, N_2, N_1O_1 and O_1) detected in the whole crude oil analysis.

(+) ESI. Here, it is the neutral nitrogen (pyrrolic species) fraction for (−) ESI. As the fractionation continues to the basic nitrogen fraction, the least sterically hindered (lowest degree of alkylation) pyrrolic species elute (N_1 class) along with their thiophenic sulfur-containing analogues (N_1S_1) class. These 2 classes reside on, or immediately adjacent to the polycyclic aromatic hydrocarbons (PAH) line and are thus bare, or near bare, pyrrolic aromatic cores.[46,74,75] The polar polyfunctional nitrogen species (N_2 and N_1O_1 data) begin to dominate, and account for ~50% of the total relative ion abundance. Although N_2 and N_1O_1 constitute ~22% of the total relative ion abundance, other polyfunctional species, such as N_2S_1, $N_1O_1S_1$, N_2O_1, and N_1O_2 contribute to the remainder (data not shown). The trend continues into the polars fraction, for which polar polyfunctional species that contain 2 or more N or O heteroatoms account for nearly 65% of the total relative abundance.

The deactivated silicic acid column chromatography method discussed above enables the coarse separation of the 2 dominant forms of nitrogen (pyridinic and

pyrrolic) in petroleum by carbon number, DBE (aromaticity), and polarity, and is therefore better suited for subsequent MS analysis. It achieves the separation through interaction of the nitrogen functionality with the stationary phase. As a result, the most sterically hindered nitrogen-containing species (highest carbon number) elute first and the carbon numbers decline as the separation proceeds. The most strongly retained species elute in the latter 2 fractions (basic N and polars), for which lower-abundance polyfunctional species in the whole crude oil begin to emerge. The greatest difference in this elution window is evident in the mono-functional basic nitrogen species, which continue to elute into the polar fraction. The weaker interaction between the stationary phase and pyrrolic nitrogen species terminates their elution in the basic nitrogen fraction, and polyfunctional species dominate the polars fraction. Analysis of the fractions by both (+) and (−) ESI FT-ICR MS reveals selective ionization, because there are defined monomer ion yield trends and similarity between the whole crude and specific fractions that depend on the ionization mode. Simply, the basic nitrogen fraction from (+) ESI and the neutral nitrogen fraction from (−) ESI are similar to the whole crude results. To further investigate the carbon number dependence of selective ionization, we revisit the modified aminopropyl silica (MAPS) fractionation of MacKay bitumen,[52] which enables separation by molecular weight (carbon number).

Naphthenic acid characterization by MAPS fractionation and (−) ESI FT-ICR MS

The MAPS fractionation procedure first isolates acidic species through their interaction with the amino functionality of the stationary phase. However, once isolated, the solvent system is changed from normal to reversed-phase, and the retained acids then elute by hydrophobicity through their interaction with the propyl functionality of the stationary phase. The retained acids are therefore separated into fractions of increasing carbon number, and thus the separation allows for further investigation of the carbon number dependence of selective ionization (ionization efficiency/monomer ion yield). Fig. 4 summarizes the mass spectral analysis of the whole bitumen APS extract (top), *versus* the MAPS fractions (MA1–MA6, bottom). The MAPS fractionation method clearly extends the detected molecular weight range, as MAPS fractions MA5 and MA6 extend well beyond 1 kDa. The monomer ion yield (ionization efficiency) data for the whole APS bitumen extract and all MAPS fractions are presented in Fig. 5. As the fraction-ation progresses, the molecular weight also increases. However, the monomer ion yield data precipitously decreases and reaches a value 80-fold less for MA5 than for MA1. MA5 and MA6 performed so poorly in the standard NH_4OH modified toluene : methanol solvent systems commonly used for (−) ESI analysis, that MA5 required the use of twice the normal volume of NH_4OH, and MA6 required elimination of toluene and NH_4OH, and replacement with dichloromethane and TMAH for successful analysis. Despite these efforts, the monomer ion yield is still ~25× less than for the MA1 fraction, and is thus presented for comparison purposes only. The monomer ion yield for the whole bitumen APS extract is roughly the average of that for MA1–MA3, and the mass spectrum spans a similar molecular weight range and chemical composition (dominated by the O_2 class) of these 3 fractions. Thus, as for the pyridinic and pyrrolic nitrogen results, higher molecular weight (higher carbon number) species appear to ionize less efficiently (lower monomer ion yield) than their lower molecular weight forms. The exact
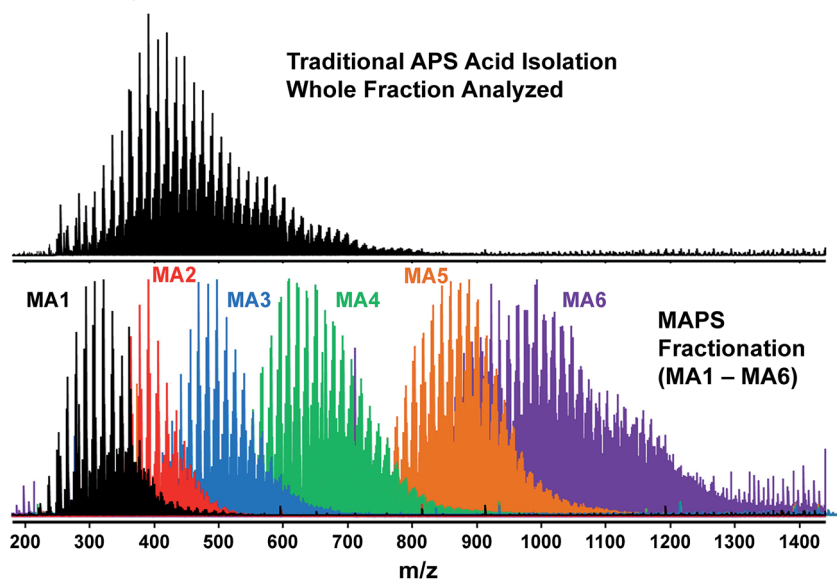
APS versus MAPS Fractionation of Bitumen

Fig. 4 Broadband (−) ESI FT-ICR mass spectrum of the aminopropyl silica combined acids extract obtained from MacKay bitumen (top). Broadband (−) ESI FT-ICR mass spectra of the modified aminopropyl silica extracts (MA1 (black)−MA6 (purple)) obtained from MacKay bitumen (bottom).

reason is currently unknown, but clues are provided from the analysis of ultra-complex asphaltene samples by APPI FT-ICR MS (see below).

Asphaltene characterization *via* extrography fractionation and +APPI FT-ICR MS

The mass spectral analysis of asphaltenes has been plagued by difficulties for decades.[39,47,53,76–79] Most notably, the H : C ratio of species readily observed based on mass spectrometry (H : C $\sim$ 0.8) is much lower than that obtained *via* bulk
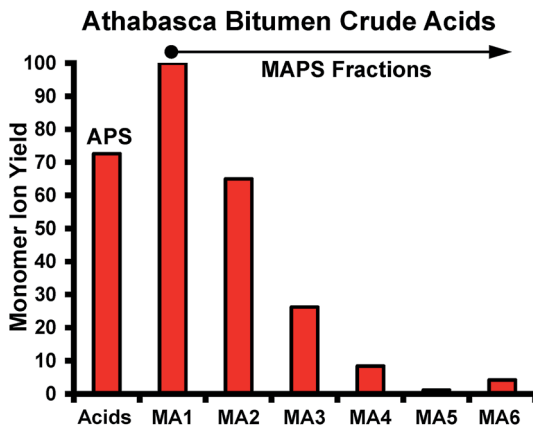

Fig. 5 Monomer ion yield for the seven mass spectra presented in Fig. 4. The whole deasphalted oil APS extract is on the left, and is followed by MAPS fractions MA1−MA6.

analysis (H : C ~1.0–1.1), and the mass spectral decomposition products obtained from tandem MS experiments did not match thermal decomposition products observed in lab-based experiments or readily encountered in normal refinery operations.[47,80–87] Thus, it was obvious that some form of selective ionization influences not only the observed H : C ratio, but also the accessible structures. Briefly, multiple reports of tandem MS results of unfractionated asphaltenes yielded simple dealkylation products (with no change in the precursor ion DBE), strongly suggesting that the dominant asphaltene structural motif is a single, alkyl-substituted aromatic core (known as the island motif).[87–89] However, multiple other reports contradicted those findings and suggested that the dominant motif was composed of multiple aromatic cores linked by alkyl or cycloalkyl groups (known as the archipelago motif).[39,81,90–92] Irrespective of the conflicting reports, it is readily apparent that the mass spectral analysis of asphaltenes suffers from selective ionization, and the species readily ionized have H : C ratios of ~0.8, corresponding to 3–9 ring aromatics with a very low degree of alkyl substitution (0–14 CH_2 groups).[40,47,93,94] Recently, a three-part series of manuscripts investigated the selective ionization of asphaltenes and proposed an extrography fractionation method to reduce its impact on the mass spectral
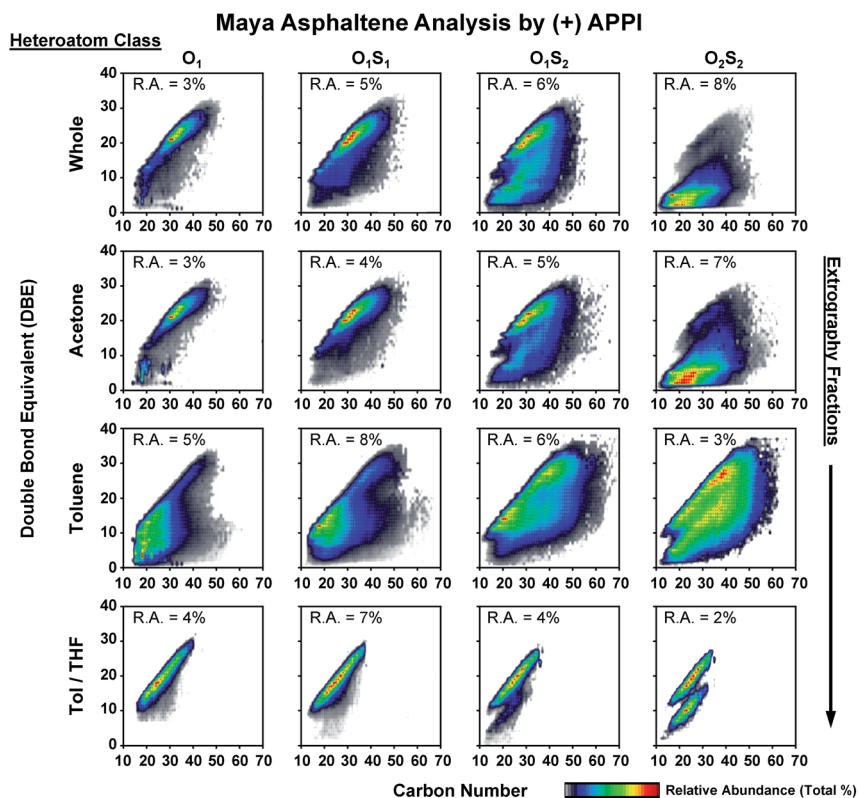

Fig. 6 Isoabundance-contoured plots of DBE *versus* carbon number from the (+) APPI FT-ICR MS analysis of the whole Maya crude oil asphaltene fraction and its acetone, toluene, and toluene/THF fractions obtained *via* extrography fractionation for the 4 heteroatom classes (O_1, O_1S_1, O_1S_2, and O_2S_2).
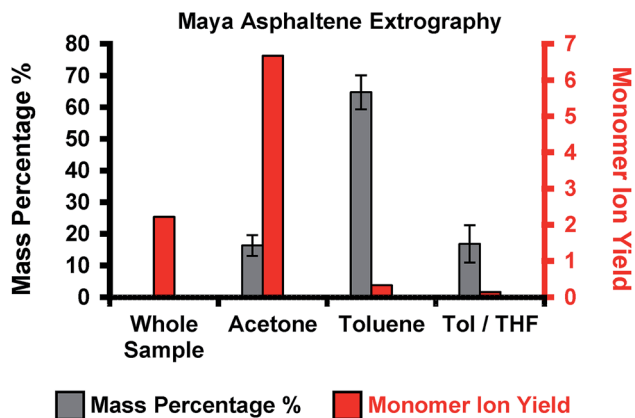
Fig. 7 Mass distribution (left) and monomer ion yield (right) for the extrography asphaltene fractionation for Maya asphaltenes.

analysis.[53,54,57] Fig. 6 provides further evidence of its success for APPI FT-ICR MS analysis of a whole Maya asphaltene and its associated acetone, toluene, and toluene/tetrahydrofuran extrography fractions collected from a simplified version (3 fractions instead of the original 8 fractions) of the previously reported method.[54] Results for the O_1, O_1S_1, O_1S_2, and O_2S_2 classes are presented for the whole asphaltene and 3 extrography fractions. Comparison of the whole asphaltene data to that obtained for the acetone fraction reveals striking similarity and exposes the problem of selective ionization in asphaltene analyses. Simply, as highlighted in Fig. 7, the acetone fraction is only 16% wt of the whole asphaltene, but ionizes 20× more efficiently than the toluene fraction (~65% wt) and 45× more efficiently than the toluene/THF fraction (17% wt). Thus, analysis of the whole asphaltene sample captures the compositional information of only 16% wt of the entire sample, and thereby fails to account for the species highlighted in the toluene and toluene/THF fractions that account for 80+% wt of the asphaltene sample. The proposed reason behind the large differences in monomer ion yield was suggested to be the effects of aggregation, because the precipitated mass *versus* heptane dilution yielded dramatic differences between the two end members in monomer ion yield (acetone and toluene/THF fractions).[54,57] At 40% vol heptane into a toluene solution, only ~5 wt% of the acetone fraction precipitated, whereas more than 90 wt% of the toluene/THF fraction precipitated. The difference in ionization efficiency also appears to be linked to molecular structure, as the dominant structural motif in this and other asphaltene acetone extrography fractions is the island motif. Conversely, the dominant structural motif in this and other asphaltene toluene and toluene/THF extrography fractions is the archipelago motif. Although convincing and correlated with monomer ion yield data for a handful of samples, the impact of aggregation in complex matrices appears to be very important, and warrants future study.

Conclusions

The compositional complexity of crude oils requires a separation method that can generate manageable fractions that can be selectively characterized based on the

ionization method, analyte functional group(s), aromaticity, and molecular weight. The silicic acid separation method successfully addresses the separation and targeted ionization of pyridinic ((+) ESI) and pyrrolic ((−) ESI) nitrogen-containing species, but exposes the preferential ionization of lower molecular weight pyridinic and pyrrolic species at the expense of higher molecular weight species. The monomer ion yields for the basic nitrogen fractions, combined with the similarity between the whole sample results and those of the basic nitrogen fraction ((+) ESI) and neutral nitrogen fraction ((−) ESI), strongly suggest that selective ionization is a major problem for the comprehensive characterization of complex samples based on direct "dilute and shoot" analyses. Selective isolation of acidic species by aminopropyl silica and subsequent analysis of the whole acid extract revealed identical selective ionization issues (for acids) compared to the MAPS fractions for the same extract (further separated by hydrophobicity (carbon number)). Ionization favors the lowest molecular weight species over higher molecular weight species, as exemplified by up to 80-fold+ difference in monomer ion yield for the later eluting (higher molecular weight) species. Finally, we revisited selective ionization in an ultra-complex asphaltene fraction isolated from Maya crude oil. Consistent with similar analyses, mass spectral analysis of the whole (unfractionated) asphaltene yielded results nearly identical to those for the acetone extrography fraction, which had a monomer ion yield 20-fold higher than the next eluting fraction (toluene) but comprised only 16% wt of the whole sample. Previous reports have linked this selective ionization to aggregation, and given the present results for nitrogen-containing (pyridinic and pyrrolic), oxygen-containing (carboxylic acids), and oxygen and sulfur-containing (OxSy) species, the link(s) between structure, carbon number, aggregation tendency, and monomer ion yield require(s) further research.

Conflicts of interest

There are no conflicts to declare.

Acknowledgements

References

1 A. G. Marshall and R. P. Rodgers, Petroleomics: The Next Grand Challenge For Chemical Analysis, *Acc. Chem. Res.*, 2004, **37**, 53–59.

2 L. C. Krajewski, R. P. Rodgers and A. G. Marshall, 126264 Assigned Chemical Formulas from an Atmospheric Pressure Photoionization 9.4 T Fourier Transform Positive Ion Cyclotron Resonance Mass Spectrum, *Anal. Chem.*, 2017, **89**, 11318–11324.

3 Y. E. Corilo, B. G. Vaz, R. C. Simas, H. D. Lopes Nascimento, C. F. Klitzke, R. C. L. Pereira, W. L. Bastos, E. V. Santos Neto, R. P. Rodgers and M. N. Eberlin, Petroleomics by ESI(±) FT-ICR MS, *Anal. Chem.*, 2010, **82**(10), 3990–3996.

4 P. L. Grizzle and D. M. Sablotny, Automated Liquid Chromatographic Compound Class Group-Type Separation of Crude Oils and Bitumens Using Chemically Bonded Aminosilane, *Anal. Chem.*, 1986, **58**, 2389–2396.

5 A. M. McKenna, J. M. Purcell, R. P. Rodgers and A. G. Marshall, Heavy Petroleum Composition. 1. Exhaustive Compositional Analysis of Athabasca Bitumen HVGO Distillates by Fourier Transform Ion Cyclotron Resonance Mass Spectrometry: A Definitive Test of the Boduszynski Model, *Energy Fuels*, 2010, **24**(5), 2929–2938.

6 A. M. McKenna, G. T. Blakney, F. Xian, P. B. Glaser, R. P. Rodgers and A. G. Marshall, Heavy Petroleum Composition. 2. Progression of the Boduszynski Model to the Limit of Distillation by Ultrahigh-Resolution FT-ICR Mass Spectrometry, *Energy Fuels*, 2010, **24**(5), 2939–2946.

7 B. M. F. Ávila, B. G. Vaz, R. Pereira, A. O. Gomes, R. C. L. Pereira, Y. E. Corilo, R. C. Simas, H. D. L. Nascimento, M. N. Eberlin and D. A. Azevedo, Comprehensive Chemical Composition of Gas Oil Cuts Using Two-Dimensional Gas Chromatography with Time-of-Flight Mass Spectrometry and Electrospray Ionization Coupled to Fourier Transform Ion Cyclotron Resonance Mass Spectrometry, *Energy Fuels*, 2012, **26**(8), 5069–5079.

8 A. Gaspar, E. Zellermann, S. Lababidi, J. Reece and W. Schrader, Impact of Different Ionization Methods on the Molecular Assignments of Asphaltenes by FT-ICR Mass Spectrometry, *Anal. Chem.*, 2012, **84**, 5257–5267.

9 Y. Cho, J. Na, N. Nho, S. Kim and S. Kim, Application of Saturates, Aromatics, Resins, Asphaltenes Crude Oil Fractionation for Detailed Chemical Characterization of Heavy Crude Oils by Fourier Transform Ion Cyclotron Resonance Mass Spectrometry Equipped with Atmospheric Pressure Photoionization, *Energy Fuels*, 2012, **26**, 2558–2565.

10 G. C. Klein, A. Angstro, R. P. Rodgers and A. G. Marshall, Use of Saturates/Aromatics/Resins/Asphaltenes (SARA) Fractionation To Determine Matrix Effects in Crude Oil Analysis by Electrospray Ionization Fourier Transform Ion Cyclotron Resonance Mass Spectrometry, *Energy Fuels*, 2006, **20**(10), 668–672.

11 D. Giraldo-Dávila, M. L. Chacón-Patiño, J. A. Orrego-Ruiz, C. Blanco-Tirado and M. Y. Combariza, Improving Compositional Space Accessibility in (+) APPI FT-ICR Mass Spectrometric Analysis of Crude Oils by Extrography and Column Chromatography Fractionation, *Fuel*, 2016, **185**, 45–58.

12 B. M. Ruddy, C. L. Hendrickson, R. P. Rodgers and A. G. Marshall, Positive Ion Electrospray Ionization Suppression in Petroleum and Complex Mixtures, *Energy Fuels*, 2018, **32**, 2901–2907.

13 J. D. McLean and P. K. Kilpatrick, Comparison of Precipitation and Extrography in the Fractionation of Crude Oil Residua, *Energy Fuels*, 1997, **11**(3), 570–585.

14 W. K. Robbins and F. C. McElroy, Systematic Evaluation and Development of Adsorption Chromatographic Techniques for Coal Liquid Analyses, *Liq. Fuels Technol.*, 1984, **2**(2), 113–154.

15 R. P. Rodgers, T. Schaub and A. G. Marshall, Petroleomics: MS Returns to Its Roots, *Anal. Chem.*, 2005, **77**(1), 20A–27A.

16 C. S. Hsu, K. Qian and W. K. Robbins, Nitrogen Speciation of Polar Petroleum Compounds by Compound Class Separation and On-Line Liquid

Chromatography - Mass Spectrometry (LC-MS), *J. High Resolut. Chromatogr.*, 1994, **17**, 271–276.

17 M. M. Boduszynski, Composition of Heavy Petroleums. 1. Molecular Weight, Hydrogen Deficiency, and Heteroatom Concentration as a Function of Atmospheric Equivalent Boiling Point up to 1400 °F (760 °C), *Energy Fuels*, 1987, **1**(1), 2–11.

18 M. M. Boduszynski, Composition of Heavy Petroleums. 2. Molecular Characterization, *Energy Fuels*, 1988, **2**(5), 2–11.

19 M. M. Boduszynski and K. H. Altgelt, Composition of Heavy Petroleums. 4. Significance of the Extended Atmospheric Equivalent Boiling-Point (AEBP) Scale, *Energy Fuels*, 1992, **6**(1), 72–76.

20 G. C. Klein, R. P. Rodgers, M. A. G. Teixeira, A. M. R. F. Teixeira and A. G. Marshall, Petroleomics: Electrospray Ionization FT-ICR Mass Analysis of NSO Compounds for Correlation Between Total Acid Number, Corrosivity, and Elemental Composition, *Preprints of Symposia*, American Chemical Society, Division of Fuel Chemistry, 2003, vol. 48, ch. 1, pp. 14–15.

21 C. A. Hughey, R. P. Rodgers, A. G. Marshall, C. C. Walters, K. Qian and P. Mankiewicz, Acidic and Neutral Polar NSO Compounds in Smackover Oils of Different Thermal Maturity Revealed by Electrospray High Field Fourier Transform Ion Cyclotron Resonance Mass Spectrometry, *Org. Geochem.*, 2004, **35**(7), 863–880.

22 M. P. Barrow, J. V. Headley, K. M. Peru and P. J. Derrick, Data Visualization for the Characterization of Naphthenic Acids within Petroleum Samples, *Energy Fuels*, 2009, **23**(5), 2592–2599.

23 G. C. Klein, S. Kim, R. P. Rodgers, A. G. Marshall, A. Yen and S. Asomaning, Mass Spectral Analysis of Asphaltenes. I. Compositional Differences between Pressure-Drop and Solvent-Drop Asphaltenes Determined by Electrospray Ionization Fourier Transform Ion Cyclotron Resonance Mass Spectrometry, *Energy Fuels*, 2006, **20**(9), 1965–1972.

24 Q. Shi, S. Zhao, Z. Xu, K. H. Chung, Y. Zhang and C. Xu, Distribution of Acids and Neutral Nitrogen Compounds in a Chinese Crude Oil and Its Fractions: Characterized by Negative-Ion Electrospray Ionization Fourier Transform Ion Cyclotron Resonance Mass Spectrometry, *Energy Fuels*, 2010, **24**(7), 4005–4011.

25 X. Zhu, Q. Shi, Y. Zhang, N. Pan, C. Xu, K. H. Chung and S. Zhao, Characterization of Nitrogen Compounds in Coker Heavy Gas Oil and Its Subfractions by Liquid Chromatographic Separation Followed by Fourier Transform Ion Cyclotron Resonance Mass Spectrometry, *Energy Fuels*, 2011, **25**(1), 281–287.

26 J. A. Valencia-dávila, M. Witt, C. Blanco-tirado and M. Y. Combariza, Molecular Characterization of Naphthenic Acids from Heavy Crude Oils Using MALDI FT-ICR Mass Spectrometry, *Fuel*, 2018, **231**(February), 126–133.

27 P. V. Hemmingsen, S. Kim, H. E. Pettersen, R. P. Rodgers, J. Sjöblom and A. G. Marshall, Structural Characterization and Interfacial Behavior of Acidic Compounds Extracted from a North Sea Oil, *Energy Fuels*, 2006, **20**(5), 1980–1987.

28 A. C. Clingenpeel, T. R. Fredriksen, K. Qian and M. R. Harper, Comprehensive Characterization of Petroleum Acids by Distillation, Solid Phase Extraction Separation, and Fourier Transform Ion Cyclotron Resonance Mass Spectrometry, *Energy Fuels*, 2018, **32**, 9271–9279.

29 A. Alvarez-majmutov, R. Gieleciak and J. Chen, Modeling the Molecular Composition of Vacuum Residue from Oil Sand Bitumen, *Fuel*, 2019, **241**, 744–752.

30 M. M. Boduszynski, R. J. Hurtubise, T. W. Allen and H. F. Silver, Determination of Hydrocarbon Composition in High-Boiling and Nondistillable Coal Liquids by Liquid-Chromatography Field-Ionization Mass-Spectrometry, *Anal. Chem.*, 1983, **55**(2), 232–241.

31 M. M. Boduszynski, Asphaltenes in Petroleum Asphalts. Composition and Formation, in *Chemistry of Asphaltenes*, American Chemical Society, Washington, D.C., USA, 1982, pp. 119–135.

32 M. M. Boduszynski, R. J. Hurtubise and H. F. Silver, Separation of Solvent-Refined Coal Into Compound-Class Fractions, *Anal. Chem.*, 1982, **54**(3), 375–381.

33 M. Li, S. R. Larter, D. Stoddart and M. Bjoroy, Liquid Chromatographic Separation Schemes for Pyrrole and Pyridine Nitrogen Aromatic Heterocycle Fractions from Crude Oils Suitable for Rapid Characterization of Geochemical Samples, *Anal. Chem.*, 1992, **64**(14), 1337–1344.

34 B. Bennett and G. D. Love, Release of Organic Nitrogen Compounds from Kerogen via Catalytic Hydropyrolysis, *Geochem. Trans.*, 2000, **1**, 61–67.

35 G. F. Bolshakov, Organic Sulfur Compounds of Petroleum, *Sulfur Rep.*, 1986, **5**(2), 103–393.

36 V. V. Lobodin, W. K. Robbins, J. Lu and R. P. Rodgers, Separation and Characterization of Reactive and Non-Reactive Sulfur in Petroleum and Its Fractions, *Energy Fuels*, 2015, **29**(10), 6177–6186.

37 P. Liu, Q. Shi, N. Pan, Y. Zhang, K. H. Chung, S. Zhao and C. Xu, Distribution of Sulfides and Thiophenic Compounds in VGO Subfractions: Characterized by Positive-Ion Electrospray Fourier Transform Ion Cyclotron Resonance Mass Spectrometry, *Energy Fuels*, 2011, **25**(7), 3014–3020.

38 L. R. Snyder, Petroleum Nitrogen Compounds and Oxygen Compounds, *Acc. Chem. Res.*, 1970, **3**(9), 290–299.

39 M. Gray, R. Tykwinski, J. Stryker and X. Tan, Supramolecular Assembly Model for Aggregation of Petroleum Asphaltenes, *Energy Fuels*, 2011, **25**, 3125–3134.

40 J. M. Purcell, I. Merdrignac, R. P. Rodgers, A. G. Marshall, T. Gauthier and I. Guibard, Stepwise Structural Characterization of Asphaltenes during Deep Hydroconversion Processes Determined by Atmospheric Pressure Photoionization (APPI) Fourier Transform Ion Cyclotron Resonance (FT-ICR) Mass Spectrometry, *Energy Fuels*, 2010, **24**(4), 2257–2265.

41 D. Giraldo-Dávila, M. L. Chacón-Patiño, A. M. McKenna, C. Blanco-Tirado and M. Y. Combariza, Correlations Between Molecular Composition and the Adsorption, Aggregation and Emulsifying Behavior of Petrophase 2017 Asphaltenes and Their TLC Fractions, *Energy Fuels*, 2018, **32**(3), 2769–2780.

42 E. Rogel, C. Ovalles and M. Moir, Asphaltene Chemical Characterization as a Function of Solubility: Effects on Stability and Aggregation, *Energy Fuels*, 2012, **26**(5), 2655–2662.

43 E. Rogel and M. Witt, Atmospheric Pressure Photoionization Coupled to Fourier Transform Ion Cyclotron Resonance Mass Spectrometry To Characterize Asphaltene Deposit Solubility Fractions: Comparison to Bulk Properties, *Energy Fuels*, 2016, **30**, 915–923.

44 R. P. Rodgers and A. G. Marshall, Petroleomics: Advanced Characterization of Petroleum-Derived Materials by Fourier Transform Ion Cyclotron Resonance Mass Spectrometry (FT-ICR MS), in *Asphaltenes, Heavy Oils, and Petroleomics*, ed. O. C. Mullins, E. Y. Sheu, A. Hammam and A. G. Marshall, Springer, 2007, pp. 63–93.

45 C. L. Hendrickson, J. P. Quinn, N. K. Kaiser, D. F. Smith, G. T. Blakney, T. Chen, A. G. Marshall, C. R. Weisbrod and S. C. Beu, 21 Tesla Fourier Transform Ion Cyclotron Resonance Mass Spectrometer: A National Resource for Ultrahigh Resolution Mass Analysis, *J. Am. Soc. Mass Spectrom.*, 2015, **26**(9), 1626–1632.

46 Y. Cho, Y. H. Kim and S. Kim, Planar Limit-Assisted Structural Interpretation of Saturates/Aromatics/Resins/Asphaltenes Fractionated Crude Oil Compounds Observed by Fourier Transform Ion Cyclotron Resonance Mass Spectrometry, *Anal. Chem.*, 2011, **83**(15), 6068–6073.

47 A. M. McKenna, A. G. Marshall and R. P. Rodgers, Heavy Petroleum Composition. 4. Asphaltene Compositional Space, *Energy Fuels*, 2013, **27**, 1257–1267.

48 A. M. Wittrig, T. R. Fredriksen, K. Qian, A. C. Clingenpeel and M. R. Harper, Single Dalton Collision-Induced Dissociation for Petroleum Structure Characterization, *Energy Fuels*, 2017, **31**(12), 13338–13344.

49 C. P. Rüger, C. Grimmer, M. Sklorz, A. Neumann, T. Streibel and R. Zimmermann, Combination of Different Thermal Analysis Methods Coupled to Mass Spectrometry for the Analysis of Asphaltenes and Their Parent Crude Oils: Comprehensive Characterization of the Molecular Pyrolysis Pattern, *Energy Fuels*, 2017, **32**(3), 2699–2711.

50 C. P. Rüger, T. Miersch, T. Schwemer, M. Sklorz and R. Zimmermann, Hyphenation of Thermal Analysis to Ultrahigh-Resolution Mass Spectrometry (Fourier Transform Ion Cyclotron Resonance Mass Spectrometry) Using Atmospheric Pressure Chemical Ionization For Studying Composition and Thermal Degradation of Complex Materials, *Anal. Chem.*, 2015, **87**(13), 6493–6499.

51 C. P. Rüger, A. Neumann, M. Sklorz, T. Schwemer and R. Zimmermann, Thermal Analysis Coupled to Ultrahigh Resolution Mass Spectrometry with Collision Induced Dissociation for Complex Petroleum Samples: Heavy Oil Composition and Asphaltene Precipitation Effects, *Energy Fuels*, 2017, **31**, 13144–13158.

52 S. M. Rowland, W. K. Robbins, Y. E. Corilo, A. G. Marshall and R. P. Rodgers, Solid-Phase Extraction Fractionation To Extend the Characterization of Naphthenic Acids in Crude Oil by Electrospray Ionization Fourier Transform Ion Cyclotron Resonance Mass Spectrometry, *Energy Fuels*, 2014, **28**, 5043–5048.

53 M. L. Chacón-Patiño, S. M. Rowland and R. P. Rodgers, Advances in Asphaltene Petroleomics. Part 1: Asphaltenes Are Composed of Abundant Island and Archipelago Structural Motifs, *Energy Fuels*, 2017, **31**(12), 13509–13518.

54 M. L. Chacón-Patiño, S. M. Rowland and R. P. Rodgers, Advances in Asphaltene Petroleomics. Part 2: Selective Separation Method That Reveals Fractions Enriched in Island and Archipelago Structural Motifs by Mass Spectrometry, *Energy Fuels*, 2018, **32**(1), 314–328.

55 G. A. Vasconcelos, R. C. L. Pereira, C. D. F. Santos, V. V. Carvalho, L. V. Tose, W. Romão and B. G. Vaz, Extraction and Fractionation of Basic Nitrogen Compounds in Vacuum Residue by Solid-Phase Extraction and Characterization by Ultra-High Resolution Mass Spectrometry, *Int. J. Mass Spectrom.*, 2017, **418**, 67–72.

56 C. S. Hsu, K. Qian, T. Aczel, S. C. Blum, W. N. Olmstead, L. H. Kaplan, W. K. Robbins, W. W. Schulz and M. A. McLean, On-Line Liquid Chromatography/Mass Spectrometry for Heavy Hydrocarbon Characterization, *Energy Fuels*, 1991, **5**(3), 395–398.

57 M. L. Chacón-Patiño, S. M. Rowland and R. P. Rodgers, Advances in Asphaltene Petroleomics. Part 3. Dominance of Island or Archipelago Structural Motif Is Sample Dependent, *Energy Fuels*, 2018, **32**(9), 9106–9120.

58 L. Nyadong, J. Lai, C. Thompsen, C. J. LaFrancois, X. Cai, C. Song, J. Wang and W. Wang, High-Field Orbitrap Mass Spectrometry and Tandem Mass Spectrometry for Molecular Characterization of Asphaltenes, *Energy Fuels*, 2018, **32**(1), 294–305.

59 O. P. Strausz, A. Morales-Izquierdo, N. Kazmi, D. S. Montgomery, J. D. Payzant, I. Safarik and J. Murgich, Chemical Composition of Athabasca Bitumen: The Saturate Fraction, *Energy Fuels*, 2010, **24**(9), 5053–5072.

60 K. Qian, W. K. Robbins, C. A. Hughey, H. J. Cooper, R. P. Rodgers and A. G. Marshall, Resolution and Identification of Elemental Compositions for More than 3000 Crude Acids in Heavy Petroleum by Negative-Ion Microelectrospray High-Field Fourier Transform Ion Cyclotron Resonance Mass Spectrometry, *Energy Fuels*, 2001, **15**(6), 1505–1511.

61 W. E. Rudzinski, L. Oehlers, Y. Zhang and B. Najera, Tandem Mass Spectrometric Characterization of Commercial Naphthenic Acids and a Maya Crude Oil, *Energy Fuels*, 2002, **16**(5), 1178–1185.

62 M. L. Chacón-Patiño, S. J. Vesga-Martínez, C. Blanco-Tirado, J. A. Orrego-Ruiz, A. Gómez-Escudero and M. Y. Combariza, Exploring Occluded Compounds and Their Interactions with Asphaltene Networks Using High-Resolution Mass Spectrometry, *Energy Fuels*, 2016, **30**(6), 4550–4561.

63 G. C. Klein, S. Kim, R. P. Rodgers, A. G. Marshall and A. Yen, Mass Spectral Analysis of Asphaltenes. II. Detailed Compositional Comparison of Asphaltenes Deposit to Its Crude Oil Counterpart for Two Geographically Different Crude Oils by ESI FT-ICR MS, *Energy Fuels*, 2006, **20**, 1973–1979.

64 V. V. Lobodin, P. Juyal, A. M. Mckenna, R. P. Rodgers and A. G. Marshall, Tetramethylammonium Hydroxide as a Reagent for Complex Mixture Analysis by Negative Ion Electrospray Ionization Mass Spectrometry, *Anal. Chem.*, 2013, **85**, 7803–7808.

65 N. K. Kaiser, J. P. Quinn, G. T. Blakney, C. L. Hendrickson and A. G. Marshall, A Novel 9.4 Tesla FT-ICR Mass Spectrometer with Improved Sensitivity, Mass Resolution, and Mass Range, *J. Am. Soc. Mass Spectrom.*, 2011, **22**(8), 1343–1351.

66 G. T. Blakney, C. L. Hendrickson and A. G. Marshall, Predator Data Station: A Fast Data Acquisition System for Advanced FT-ICR MS Experiments, *Int. J. Mass Spectrom.*, 2011, **306**(2–3), 246–252.

67 Y. E. Corilo, *PetroOrg Software*, Florida State University, All rights reserved, 2013, http://www.petroorg.com.

68 A. C. Clingenpeel, S. M. Rowland, Y. E. Corilo, P. Zito and R. P. Rodgers, Fractionation of Interfacial Material Reveals a Continuum of Acidic Species

That Contribute to Stable Emulsion Formation, *Energy Fuels*, 2017, **31**(6), 5933–5939.

69 A. C. Clingenpeel, W. K. Robbins, Y. E. Corilo and R. P. Rodgers, Effect of the Water Content on Silica Gel for the Isolation of Interfacial Material from Athabasca Bitumen, *Energy Fuels*, 2015, **29**(11), 7150–7155.

70 J. C. Putman, S. M. Rowland, D. C. Podgorski, W. K. Robbins and R. P. Rodgers, Dual-Column Aromatic Ring Class Separation with Improved Universal Detection across Mobile-Phase Gradients via Eluate Dilution, *Energy Fuels*, 2017, **31**, 12064–12071.

71 A. G. Marshall and R. P. Rodgers, Petroleomics: Chemistry of the Underworld, *Proc. Natl. Acad. Sci. U. S. A.*, 2008, **105**(47), 18090–18095.

72 H. Korsten, Characterization of Hydrocarbon Systems by DBE Concept, *AIChE J.*, 1997, **43**(6), 1559–1568.

73 F. W. McLafferty and F. Tureček, *Interpretation of Mass Spectra*, University Science Books, 4th edn, 1993, pp. 27–28.

74 V. V. Lobodin, A. G. Marshall and C. S. Hsu, Compositional Space Boundaries for Organic Compounds, *Anal. Chem.*, 2012, **84**, 3410–3416.

75 C. S. Hsu, V. V. Lobodin, R. P. Rodgers, A. M. McKenna and A. G. Marshall, Compositional Boundaries for Fossil Hydrocarbons, *Energy Fuels*, 2011, **25**, 2174–2178.

76 A. A. Herod, Limitations of Mass Spectrometric Methods for the Characterization, *Rapid Commun. Mass Spectrom.*, 2010, **24**(24), 2507–2519.

77 A. A. Herod, K. D. Bartle, T. J. Morgan and R. Kandiyoti, Analytical Methods for Characterizing High-Mass Complex Polydisperse Hydrocarbon Mixtures: An Overview, *Chem. Rev.*, 2012, **112**(7), 3892–3923.

78 A. M. McKenna, L. J. Donald, J. E. Fitzsimmons, P. Juyal, V. Spicer, K. G. Standing, A. G. Marshall and R. P. Rodgers, Heavy Petroleum Composition. 3. Asphaltene Aggregation, *Energy Fuels*, 2013, **27**(3), 1246–1256.

79 M. L. Chacón-Patiño, C. Blanco-Tirado, J. A. Orrego-Ruiz, A. Gómez-Escudero and M. Y. Combariza, High Resolution Mass Spectrometric View of Asphaltene–SiO$_2$ Interactions, *Energy Fuels*, 2015, **29**(3), 1323–1331.

80 E. Rogel and M. Witt, Atmospheric Pressure Photoionization Coupled to Fourier Transform Ion Cyclotron Resonance Mass Spectrometry to Characterize Asphaltene Deposit Solubility Fractions: Comparison to Bulk Properties, *Energy Fuels*, 2016, **30**(2), 915–923.

81 A. Karimi, K. Qian, W. N. Olmstead, H. Freund, C. Yung and M. R. Gray, Quantitative Evidence for Bridged Structures in Asphaltenes by Thin Film Pyrolysis, *Energy Fuels*, 2011, **25**, 3581–3589.

82 R. I. Rueda-Velásquez, H. Freund, K. Qian, W. N. Olmstead and M. R. Gray, Characterization of Asphaltene Building Blocks by Cracking under Favorable Hydrogenation Conditions, *Energy Fuels*, 2013, **27**, 1817–1829.

83 M. R. Gray, Consistency of Asphaltene Chemical Structures with Pyrolysis and Coking Behavior, *Energy Fuels*, 2003, **17**(6), 1566–1569.

84 M. L. Chacón-Patiño, C. Blanco-Tirado, J. A. Orrego-Ruiz, A. Gómez-Escudero and M. Y. Combariza, Tracing the Compositional Changes of Asphaltenes after Hydroconversion and Thermal Cracking Processes by High-Resolution Mass Spectrometry, *Energy Fuels*, 2015, **29**(10), 6330–6341.

85 P. E. Savage, M. T. Klein and S. G. Kukes, Petroleum Asphaltene Thermal Reaction Pathways, *Preprints of Symposia*, American Chemical Society, Division of Fuel Chemistry, 1985, vol. 30, ch. 3, pp. 408–419.

86 J. Ancheyta, F. Trejo and M. S. Rana, Definition and Structure of Asphaltenes, in *Asphaltene Chemical Transformation during Hydroprocessing of Heavy Oils*, CRC Press, Taylor & Francis Group, Boca Raton, FL, USA, 2010, pp. 1–86.

87 H. Sabbah, A. L. Morrow, A. E. Pomerantz and R. N. Zare, Evidence for Island Structures as the Dominant Architecture of Asphaltenes, *Energy Fuels*, 2011, **25**(4), 1597–1604.

88 M. R. Hurt, D. J. Borton, H. J. Choi and H. I. Kenttämaa, Comparison of the Structures of Molecules in Coal and Petroleum Asphaltenes by Using Mass Spectrometry, *Energy Fuels*, 2013, **27**(7), 3653–3658.

89 T. M. Jarrell, C. Jin, J. S. Riedeman, B. C. Owen, X. Tan, A. Scherer, R. R. Tykwinski, M. R. Gray, P. Slater and H. I. Kenttämaa, Elucidation of Structural Information Achievable for Asphaltenes via Collision-Activated Dissociation of Their Molecular Ions in MSn Experiments: A Model Compound Study, *Fuel*, 2014, **133**, 106–114.

90 Z. Liao, J. Zhao, P. Creux and C. Yang, Discussion on the Structural Features of Asphaltene Molecules, *Energy Fuels*, 2009, **23**(12), 6272–6274.

91 O. P. Strausz, T. W. Mojelsky, E. M. Lown, I. Kowalewski and F. Behar, Structural Features of Boscan and Duri Asphaltenes, *Energy Fuels*, 1999, **13**(2), 228–247.

92 J. D. Payzant, E. M. Lown and O. P. Strausz, Structural Units of Athabasca Asphaltene: The Aromatics with a Linear Carbon Framework, *Energy Fuels*, 1991, **5**(3), 445–453.

93 T. M. C. Pereira, G. Vanini, E. C. S. Oliveira, F. M. R. Cardoso, F. P. Fleming, A. C. Neto, V. Lacerda, E. V. R. Castro, B. G. Vaz and W. Romão, An Evaluation of the Aromaticity of Asphaltenes Using Atmospheric Pressure Photoionization Fourier Transform Ion Cyclotron Resonance Mass Spectrometry – APPI(±)FT-ICR MS, *Fuel*, 2014, **118**, 348–357.

94 J. S. Riedeman, N. R. Kadasala, A. Wei and H. I. Kenttämaa, Characterization of Asphaltene Deposits by Using Mass Spectrometry and Raman Spectroscopy, *Energy Fuels*, 2016, **30**(2), 805–809.